# NMR IN INCOMMENSURATE AND CHAOTIC SYSTEMS: THE DETECTION OF SOLITONS

**R. Blinc**

**J. Stefan Institute, E. Kardelj University of Ljubljana, Ljubljana, Yugoslavia**

## I. INTRODUCTION

Structural phase transitions may lead from a high temperature disordered phase with a space group $G_0$ and a unit cell edge a to:

a) A *ferrodistortive* commensurate ordered state with a space group $G_1$ and an unchanged unit cell, $a' = a$.

b) An *antiferrodistortive* commensurate ordered state with a space group $G_2$ and a unit cell size which is an integral multiple of the high temperature unit cell: $a' = m.a$, $m = 2,3,4 \ldots$

c) An *incommensurately modulated* ordered phase where the wavelength $\lambda$ of the modulation is irrational in units of the original lattice constant a: $\frac{\lambda}{a} \neq \frac{M}{N}$; M, N = 1,2, 3,4 ...
Here the translational symmetry is lost and the crystal cannot be described by any of the 230 three–dimensional crystallographic space groups though the system exhibits perfect long range order.

d) A *chaotic* state with no long range order which can in contrast to *amorphous* systems – transform itself at lower temperatures to a commensurate ordered state.

The transitions c) and d) take place when we have *deterministic* "competing interactions" and "frustration" (1); i.e. the competing structural units form a regular lattice. If the competing interactions are placed at *random* (such as in a mixed ferro–antiferroelectric crystal), a "spin glass" phase may be formed.

One of the most interesting aspects of *incommensurate* phases is the spontaneous appearance of *solitons* (2) which are arranged in a periodic lattice with a period which is irrational in units of the original lattice. The *soliton lattice* may become *chaotic* thus leading to "chaos in space" as contrasted to "chaos in time" found in dynamical systems (3).

The problems of the

i) possible existence of only a few universal routes from order to chaos in dynamical systems, and

ii) the non–linearity of the underlying natural phenomena have been extensively investigated in the last few years and are among the most outstanding open problems of condensed matter physics.

The formation of solitons in spatial structures and the routes to spatial chaos have so far received considerably less attention.

Both in dynamic and in spatial structures the soliton formation and the routes to chaos can be simulated by the onedimensional sine–Gordon equation (3) which can be written in dimensionless units as:

$$\phi_{tt} - \phi_{xx} + \sin\phi = F(x,t) - \epsilon\,\phi_t \qquad (1)$$

where $\phi_{tt} = \frac{\partial^2\phi}{\partial t^2}$, $\phi_{xx} = \frac{\partial^2\phi}{\partial x^2}$, $\phi_t = \frac{\partial\phi}{\partial t}$, $\epsilon$ is the damping parameter and F(x,t) a driving force which is in dynamical systems usually written as $\Gamma \sin(\omega_d t)$. For small $\phi$ one finds the familiar harmonic solutions. For large $\phi$ "particle–like" solitons represent exact solutions. Though the equation is completely deterministic, "chaotic" temporal response is found at large $\Gamma$ as a consequence of an interplay between an intrinsic periodic motion and an "incommensurate" external periodic perturbation. "Chaos in space" may

similarly be formed by an interplay between the period of the modulated structure and the original lattice constant which are incommensurate to each other. In the resulting "intermittent" chaotic phase the solitons are randomly pinned so that the situation in many ways corresponds to the one in "spin glasses".

Whereas magnetic resonance has been extensively used to study "ferrodistortive" and "anti–ferrodistortive" phase transitions little attention has been paid to "incommensurate" and "chaotic" type phase transitions until now. Here we shall review some recent results obtained by us in the study of:

i) The "incommensurate" and "chaotic" states in $Rb_2ZnCl_4$ and $Rb_2ZnBr_4$ with particular emphasis on the detection of solitons and the transition to chaos.

ii) Soliton–like "dynamics" in the pseudo–one dimensional antiferroelectric squaric acid, $C_4H_4O_2$.

## II. INCOMMENSURATE STATES, CHAOTIC STATES AND SOLITONS IN $Rb_2ZnCl_4$ AND $Rb_2ZnBr_4$

$Rb_2ZnCl_4$ and $Rb_2ZnBr_4$ exhibit (4) on cooling a sequence of structural phase transitions

$$P \rightarrow I \rightarrow (Ch) \rightarrow C \rightarrow C'$$

from a high temperature disordered paraelectric (P) phase to an incommensurate (I) phase followed by a – probably metastable – chaotic (Ch) phase (5) and two commensurate (C and C') ferroelectric phases.

### II.1. NMR Spectrum and Shape of the Frozen–out Modulation Wave

In translationally periodic systems the number of magnetic resonance lines in the spectrum equals to the number of physically non-equivalent nuclei per unit cell.

In incommensurate systems where the translational lattice periodicity is lost there is essentially an infinite number of nuclei which contribute to the NMR spectrum and which are equivalent to each other in the paraelectric phase. Instead of sharp lines one expects to find a frequency distribution $f(\nu)$ which reflects the spatial variation of the resonance frequencies, $\nu = \nu(x)$, which is in turn determined by the spatial variation of the frozen out modulation wave u(x):

$$\nu = \nu[u(x)] \qquad (2)$$

where

$$u(x) = A\cos[\phi(x) + \phi_o] \qquad (3)$$

in the constant amplitude approximation.

Here $\phi_o$ is an initial phase which depends on the crystal structure and is important only if $\phi(x)$ is not linear in x. The spatial variation of the phase of the modulation wave $\phi(x)$ is determined (6) in the present case by the time–independent sine–Gordon equation (1):

$$\frac{d^2\phi}{dx^2} = -\frac{n\gamma}{2\kappa} A_o^{n-2} \cdot \sin(n\phi) . \qquad (4)$$

Here $n = 6$ for $Rb_2ZnCl_4$ and $Rb_2ZnBr_4$ representing the lowest power of the "lock–in" term describing the effect of the crystal lattice, $\kappa$ is an elastic constant and the amplitude of the modulation wave varies with temperature as

$$A_o \propto (T_I - T)^{\beta} \qquad (5)$$

where $T_I$ is P–I transition temperature. Close to $T_I$ $\phi(x)$ is nearly linear in x (Fig. 1) and the modulation wave u can be described as a "plane wave". At lower temperature $\phi$ becomes non–linear in x. Nearly commensurate regions where $\phi(x) = \text{const}$ are separated by soliton–like "discommensurations" where the phase changes rapidly (Fig. 1). The phase

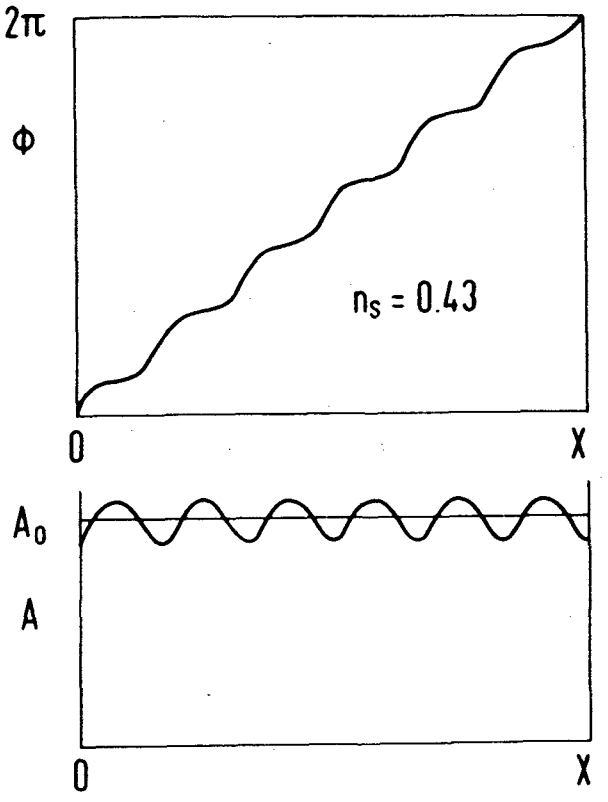


Fig. 1. Spatial variation of the phase and amplitude in an incommensurate system

solitons represent exact solutions of eq. 4 and form a regular lattice with a temperature dependent spacing $x_o$ which is generally irrational in units of the original lattice. The soliton density

$$n_s = \frac{d_o}{x_o} \qquad (6)$$

is the ratio of soliton width $d_o$ to the inter–soliton distance $x_o$ and measures the volume fraction of the crystal occuppied by the phase soliton domain walls. It is 1 in the plane wave limit just below $T_I$ and zero at the "lock–in" transition $T_c$ where $x_o \to \infty$.

For a space varying frequency $\nu(x)$ the spectral distribution function at $\nu_o$ is given by

$$f(\nu_o) = \int \delta[\nu_o - \nu(x)]\, dx \qquad (7)$$

yielding

$$f(\nu) = \frac{\text{const}}{|d\nu/dx|} \qquad (8)$$

or explicitely (4)

$$f(\nu) = \frac{\text{const}}{|\frac{d\nu}{du}|.|\frac{du}{d\phi}|.|\frac{d\phi}{dx}|} \qquad (9)$$

The NMR line–shape thus represents an extremely sensitive local probe reflecting the spatial variations of the frozen out modulation wave.

The line–shape will be peaked whenever

i) $d\nu/du \to 0$ (10a)

ii) $du/d\phi \to 0$ (10b)

or

iii) $d\phi/dx \to 0$ (10c)

It is this last point which allows for a direct determination of the soliton density (4).

To evaluate expression 9 let us expand the relation 2 in a power series and keep for simplicity only the leading linear term :

$$\nu = \nu_o + a_1 u + \ldots = \nu_o + \nu_1 \cos[\phi(x) + \phi_o] + \ldots (11)$$

where

$$\nu_1 = a_1 A_o \propto (T_I - T)^{\beta} . \qquad (12)$$

In the above case $d\nu/du = a_1 = \text{const}$ and the singularities in $f(\nu)$ will come from the zeroes of $du/d\phi$ and $d\phi/dx$. We may now distinguish two different limits:

a) In the *"plane wave"* modulation limit

$$d\phi/dx = k_I = \text{const} \neq 0 \qquad (13)$$

and the lineshape is given by

$$f(\nu) = \frac{\text{const}}{|\sin\phi|} = \frac{\text{const}}{\sqrt{1 - X^2}} \qquad (14)$$

where $X = \frac{\nu - \nu_o}{\nu_1}$. The edge singularities corresponding to $X = \pm 1$ will occur at $\nu = \nu_o - \nu_1$

and reflect the fact that the density of states has a maximum at the extreme displacements $u = \pm A_o$ of the modulation wave. The frequency separation between the edge singularities will be proportional to the amplitude of the modulation wave, i.e. to the order parameter:

$$\Delta\nu = \nu_+ - \nu_- = 2\nu_1 \propto (T_l - T)^{\beta} \quad . \qquad (15)$$

The above line–shape 14 has been observed below $T_l$ (Fig. 2) and the critical exponent $\beta$ was determined (3) as $\beta = 0.34 \pm 0.03$.

b) In the "multi–soliton" lattice modulation limit $d\phi/dx \to 0$ in the "commensurate" regions giving rise to "commensurate" peaks in addition to the incommensurate edge singularities 14 . The "commensurate" peaks are directly related to the volume fraction $n_c$ of the "commensurate" regions in the crystal: $n_s + n_c = 1$.

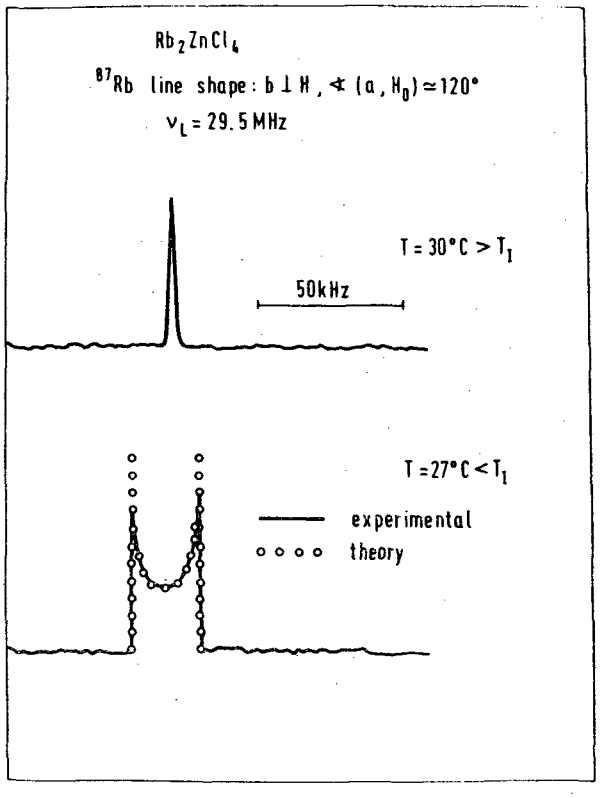


Fig. 2. $^{87}Rb$ 1/2 → − 1/2 NMR lineshape in $Rb_2ZnCl_4$ close to $T_l$

By a straightforward integration of eq. 4 we find $d\phi/dx$ so that $f(\nu)$ becomes (4)

$$f(\nu) = \frac{\text{const}}{|\sin\phi(x)|\sqrt{\Delta^2 + \cos^2[\frac{n}{2}(\phi(x) - \phi_o)]}} \, . \qquad (16)$$

The above expression is identical to eq. 4 for $\Delta \gg 1$ whereas up to n new "commensurate" lines appear for $\Delta \to 0$ (Fig. 3). The integration constant $\Delta$ is related to the soliton

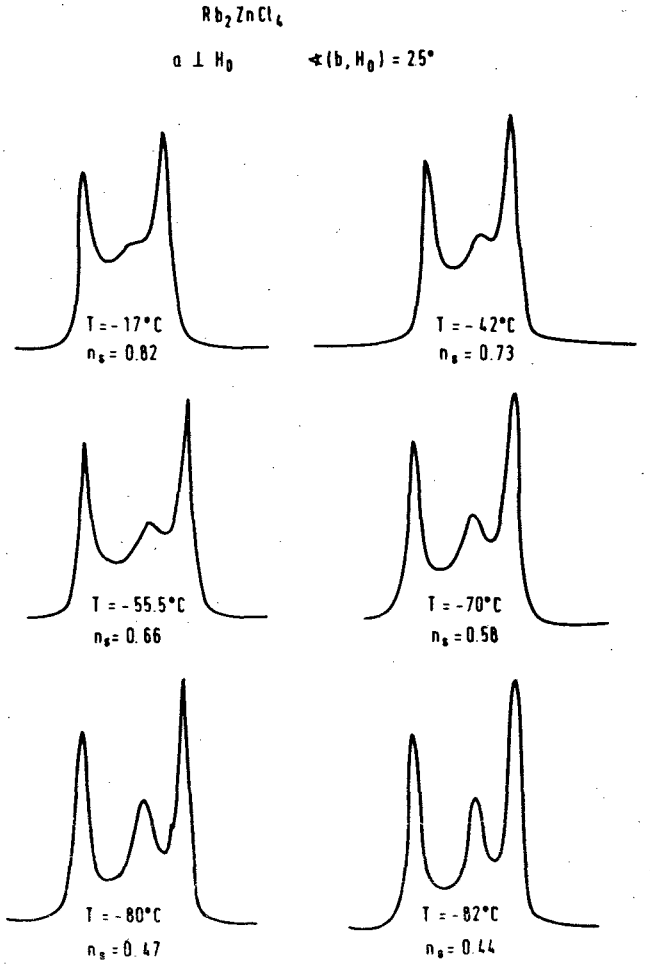


Fig. 3. $^{87}Rb$ 1/2 → − 1/2 NMR lineshape in $Rb_2ZnCl_4$ showing the appearance of the "commensurate" line as the static multi–soliton lattice becomes more pronounced.

density $n_s$ by (4):

$$n_s = \frac{\pi/2}{K(1/\sqrt{1+\Delta^2})} \qquad (17)$$

where K is the complete elliptic integral of first kind. By comparing theoretical and experimental lineshapes $\Delta$ and $n_s$ can be determined. This has been done for the $^{87}Rb$ $1/2 \rightarrow -1/2$ transition in both $Rb_2ZnCl_4$ and $Rb_2ZnBr_4$.

The temperature dependence of $n_s$ in $Rb_2ZnCl_4$ (5) is presented in Fig. 4. In evaluating $n_s$ amplitude fluctuations (6) have been as well taken into account.

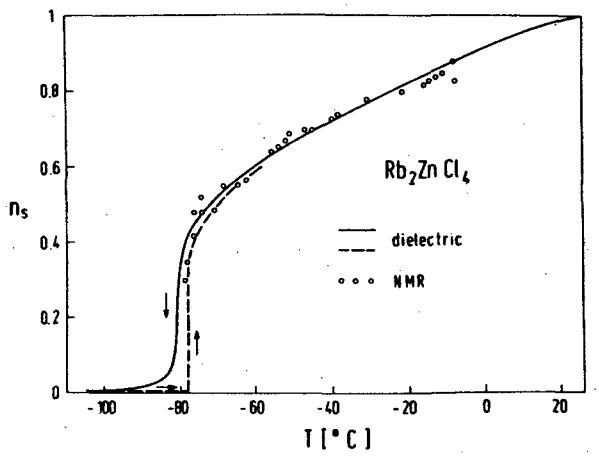


Fig. 4. Temperature dependence of the soliton density in $Rb_2ZnCl_4$

In contrast with the theoretical expectation $n_s$ is finite at $T_c$. On cooling $n_s$ is non-zero even in the C phase below $T_c$. This result can be explained by the existence of a (probably metastable) chaotic phase intermediate between the I and the C phases. In this phase the solitons are *randomly* pinned either by the coupling to the discrete lattice or by coupling to impurities and the long range order is destroyed. This result can be obtained from eq. 1 by identifying space with discrete "time" on the right hand side of this equation. The driving term F(x) is thus given by the soliton–lattice or soliton–impurity coupling which becomes the more important the closer we approach $T_c$ and the weaker is the soliton-soliton interaction. The existence of the "chaotic" phase (7) is confirmed by the anomalous broadening of the incommensurate X-ray sattelites. For $T > T_c$ the relative spread in the – uncorrelated – inter–soliton separations follows a Curie–Weiss law (8)

$$\frac{\delta x_o}{x_o} \propto \frac{1}{T - T_c}, \quad T > T_c \qquad (18)$$

but saturates at $T_c$ yielding a "chaotic" width of the X-ray incommensurate sattelite peaks (8)

$$(\delta q)_{T \leq T_c} = \text{const. } n_s \qquad (19)$$

which is proportional to the soliton density. The values of $n_s$ obtained from eq. 19 or from the dielectric data (5)

$$\chi = \chi_o + \text{const. } n_s, \quad T \leq T_c \qquad (20)$$

agree rather well with those directly determined by NMR.

Analogous results were also obtained by EPR in $K_2SeO_4$ (9).

At low enough temperatures the chaotic state disappears and we have a commensurate (C) ferroelectric phase which is again translationally invariant.

It should be noted that in the narrow multi–soliton lattice limit – where the solitons do not overlap – the NMR line-shape for randomly spaced pinned solitons

$$\langle f(\nu_o) \rangle = \left\langle \sum_i \frac{dx}{d\nu_i}\Big|_{\nu(x_i)=\nu_o} \right\rangle =$$

$$= \int dx_1 D(x_1 - x_o) \ldots \int dx_j D(x_j - jx_o) \ldots$$

$$\ldots \sum_i \frac{dx}{d\nu_i}\Big|_{\nu_i=\nu_o} \qquad (21)$$

equals to the one – $f(\nu) = \frac{dx}{d\nu}$ – for a periodic multi–soliton lattice. This is due to the fact that NMR measures just the local soliton density and is – if the solitons are

far apart – not affected by the destruction of long range order. In the above expression the position of the j–th soliton $x_j$ is determined by the distribution function $D(x_j - - jx_o)$.

II.2. Depinning of the Modulation Wave

The NMR lineshapes studies in $Rb_2ZnCl_4$ and $Rb_2ZnBr_4$ have shown that the modulation wave is generally static due to lattice or impurity pinning. The dispersion of the phason induced spin–lattice relaxation rate showed (4) that the pinning gap is of the order of 100 MHz – 1 GHz. The dependence of the maximum value of the dielectric constant on the K–content in mixed $Rb_{2x}K_{2(1-x)}ZnCl_4$ crystals as well gave a soliton–impurity pinning energy (8) of

$$U_B = 1.4 \times 10^{-5} \text{ eV} . \qquad (22)$$

In Nb $Se_3$ (10) the incommensurate charge density wave (CDW) has been depinned by an applied electric field E which was larger than a critical value $E_o$. The resulting conductivity $\sigma$ was of the form

$$\sigma = \sigma_o + \sigma_a \exp(- E/E_o) \qquad (23)$$

with the gap $E_o$ corresponding to about 0.1 K (10). For $E > E_o$ both periodic oscillations and a broad continuous noise appeared (10) signaling the approach to chaos.

In $Rb_2ZnBr_4$ thermal depinning has been observed (11) close to $T_l$.

If the modulation wave is not static the resonance frequencies are not only space but also time dependent: $\omega = \omega(x,t)$. The NMR line-shape is now given by

$$I(\omega) = \frac{1}{2\pi} \int_{-\infty}^{+\infty} G(t)\, e^{i\omega t}\, dt \qquad (24)$$

where

$$G(t) = \langle \exp[-i \int_0^t \omega(x,t')\, dt'] \rangle_x . \qquad (25)$$

i) For the case of a *uniform sliding* of the "plane wave" like modulation wave with a velocity v and a wave vector $k_l$ we have

$$u(x,t) = A \cos k_l [x + vt + \phi_o] =$$
$$= A \cos [k_l x + \Omega t + \phi_o] . \qquad (26)$$

Uniform sliding of the modulation wave thus corresponds to a harmonic oscillation of a given atom with a frequency $\Omega = k_l . v$.

Inserting eq.26 into eq.11 one can immediately obtain the autocorrelation function G(t) as:

$$G(T) = J_o[\frac{2}{w} \sin(\pi T)] \qquad (27)$$

where $J_o$ is the cylindrical Bessel function of order zero, $T = \frac{w}{2\pi} . \omega_1 t$ and $w = vk_l/\omega_1 = \Omega/\omega_1$ with $\omega_1 = 2\pi\nu_1$. For small sliding velocities where $w \ll 1$ the static lineshape is recovered:

$$I(\omega) = \frac{\text{const}}{\sqrt{1 - (\frac{\omega - \omega_o}{\omega_1})^2}}, \quad \Omega/\omega_1 \ll 1 . \qquad (28)$$

For large sliding velocities the incommensurate line broadening is motionally averaged out:

$$I(\omega) \propto \delta(\omega - \omega_o), \quad \Omega/\omega_1 \gg 1 \qquad (29)$$

and one finds just one sharp "paraelectric–like" line at $\omega_o$.

In the general case

$$I(\omega) = \sum_{n=-\infty}^{+\infty} J_n^2(\frac{1}{w})\, \delta(\frac{\omega - \omega_o}{\omega_1} - nw) \qquad (30)$$

a three component line-shape is expected with peaks around $\omega = 0$ and $\omega = \pm\omega_1$. The relative intensities of these lines and the positions of the outer peaks strongly vary with w (Fig. 5). This result is significally different from the one for "normal" motional narrowing due to a stochastic motion where G(T) is not periodic.

ii) A similar lineshape is also found for a *thermally induced floating* of a *pinned modulation* wave:

$$u = A \cos[k_l x + \psi(x,t) + \phi_o] \qquad (31)$$

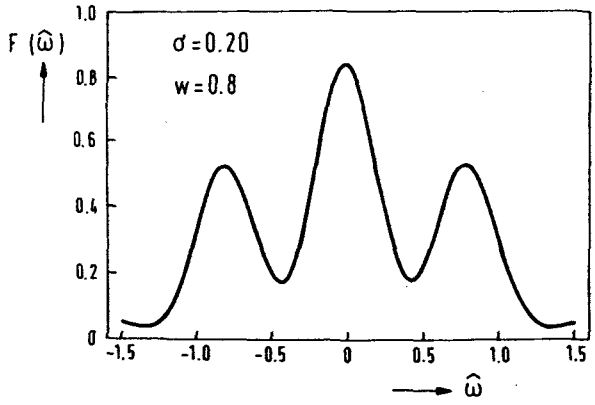


Fig. 5. NMR lineshape for a uniformly sliding modulation wave $\tilde{\omega} = (\omega - \omega_0)/\omega_1$. The line was convoluted with Gaussian of $\sigma = 0.2$.

where $\psi(x,t)$ describes the effect of pinning, e.g.:

$$\psi(x,t) = B \sin(kx) \sin(\omega t) \qquad (32)$$

and $\omega$ is the thermally excited oscillation frequency of the pinned modulation wave. B is related to the average distance between the pinning centres and is thus T–dependent. For fast oscillations $\omega/\omega_1 \gg 1$ one finds

$$I(\tilde{\omega}) = \int_0^1 \delta\{\tilde{\omega} - \cos(\pi q u + \phi_0)\, J_0[B \sin(\pi u)]\}\, du \qquad (33)$$

where $q = k_1/k$, $u = \frac{k}{\pi} . x$ and $\tilde{\omega} = \omega/\omega_1$. Depending on the value of B, a static or a motionally averaged spectrum is obtained.

Between $T_1 - 12$ K and $T_1$ the $^{87}Rb$ $1/2 \rightarrow -1/2$ NMR spectrum in $Rb_2ZnBr_4$ shows (11) in addition to the two edge singularities also a motionally averaged "central" line as predicted by eqs. 30 and 33 (Fig. 6). This demonstrates the existence of thermal depinning and phase floating at least over a part of the $Rb_2ZnBr_4$ crystal (11).

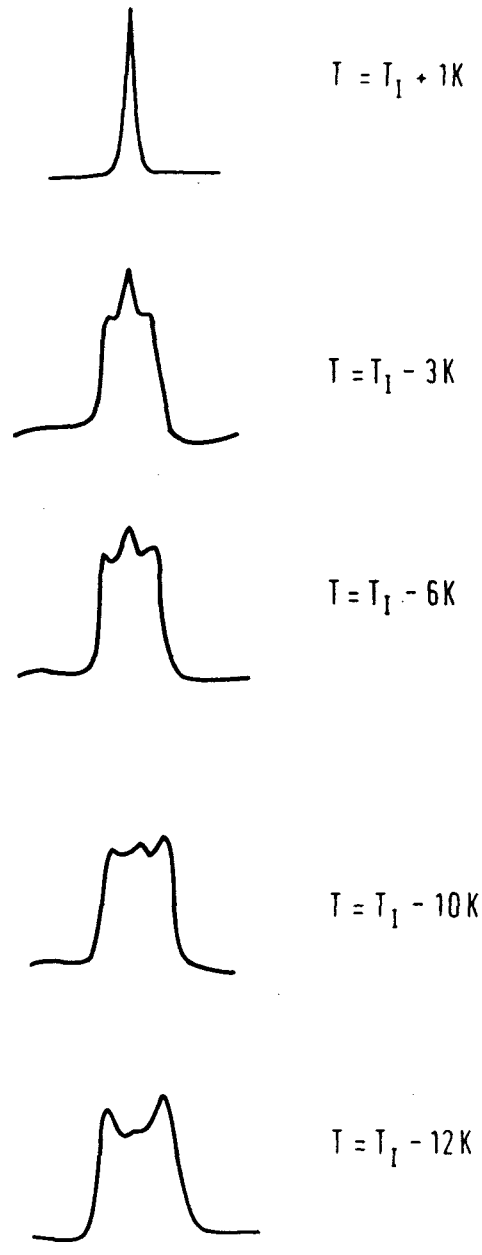


Fig. 6. $^{87}Rb$ $1/2 \rightarrow -1/2$ NMR lineshape in $Rb_2ZnBr_4$ close to $T_1$ showing motional narrowing effects due to thermal depinning and floating of the modulation wave $\nu_L = 88.3$ MHz, $\vec{a} \perp \vec{H}_0$, $\sphericalangle(\vec{c}, \vec{H}_0) = 60^\circ$.

## III. SOLITON–LIKE EXCITATIONS AND THE PHASE TRANSITION IN PSEUDO–ONE DIMENSIONAL SQUARIC ACID

Whereas solitons are part of the ground state in incommensurate systems they are entropy favoured and part of the excitation spectrum in pseudo–one dimensional ferroelectrics.

The ordered state of squaric acid, $C_4H_4O_2$, consists (12) of layers of O–H––O bonded ordered Ising chains where the Ising pseudo–spin variable ↑, ↓ refers to the two equivalent positions of the proton in the hydrogen bonds, i.e. O–H––O and O–––H–O. The O–H–––O bond length is 2.47 Å and the distance between the two proton equilibrium sites 0.44 Å as determined by the $^{17}$O–H magnetic dipolar fine structure of the naturally abundant $^{17}$O (I = 5/2) nuclear quadrupole resonance (NQR) spectra (12). For $T \ll T_c = 95°C$ the chains are completely ordered: ↑↑↑↑↑ .... As $T \to T_c$ soliton-like domain walls

↓↓↓↓|↑↑↑↑↑

start to move along the chains, resulting in a biased averaging of the $^{17}$O electric field gradient tensor:

$$V = \frac{1}{2}[1 + S(t)]\, V(^{17}O–H–––O) + \frac{1}{2}[1 - S(t)]\, V(^{17}O–––H–O).$$

Here S is the local short range order parameter at a given $^{17}$O site. At $T = T_c = 95°C$ long range order between the chains disappears and only S = S(t) remains. A $T = T_c + 15$ K the time between two successive passages of a domain wall through a given $^{17}$O site becomes of the order of the inverse splitting between the "close" and "far" – $^{17}$O–H–––O and $^{17}$O–––H–O NQR frequencies, i.e. $\sim 10^{-6}$ sec and the NQR line smears out (Fig. 7). At $T = T_c + 20$ K $S \to 0$ and one finds just the paraelectric $^{17}$O NQR frequencies though the neutron scattering data still show (12) a correlation length of about 50 unit cells along the O–H–––O bonded chains.

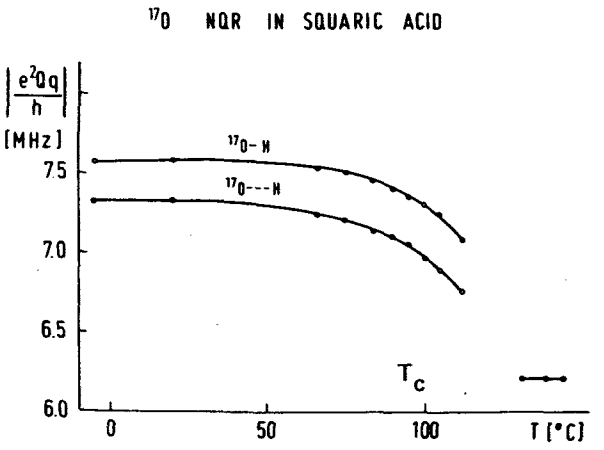


Fig. 7. Temperature dependence of the "close" ($^{17}$O–H–––O) and "far" ($^{17}$O---H–O) $^{17}$O quadrupole coupling constants in squaric acid.

### REFERENCES


1. S. Aubry, Ferroelectrics 24, 53 (1980), and references therein.
2. W.L. McMillan, Phys. Rev. B 12, 1197 (1975).
3. M.J. Feigenbaum, J. Stat. Phys. 19, 25 (1978); 21, 669 (1979); D. Bennet, A.R. Bishop and S.E. Trullinger, Z. Phys. B 74, 265 (1982); A.R. Bishop et al., Phys. Rev. Lett. 50, 1095 (1983).
4. See, for instance, R. Blinc, Physics Reports 79, 331 (1981), and references therein.
5. R. Blinc, P. Prelovšek, A. Levstik and C. Filipič, Solid State Commun. (1983), to be published.
6. R. Blinc, P. Prelovšek and R. Kind, Phys. Rev. B 27, 5404 (1983).
7. H. Mashiyama, S. Tanisaki and K. Hamano, J. Phys. Soc. Japan 50, 2139 (1981); 51, 2538 (1982). For a recent review see P. Bak, Rep. Prog. Phys. 45, 587 (1982).
8. P. Prelovšek and R. Blinc, J. Phys. C, to be published.

9. M. Fukui and R. Abe, J. Phys. Soc. Japan 51, 3942 (1982).
10. P. Monceau, paper presented at the workshop *Statics and Dynamics of Non–Linear Systems,* Erice (Italy), July 1–11, 1983, to be published by Springer Verlag.
11. R. Blinc, D. Ailion, P. Prelovšek and V. Rutar, Phys. Rev. Lett. 50, 67 (1983).
12. J. Seliger, R. Blinc and V. Žagar, J. Mag. Res. (1983), to be published.